Roadmaps with Gaps over Controllers: Achieving Efficiency in Planning under Dynamics

Aravind Sivaramakrishnan, Sumanth Tangirala, Edgar Granados, Noah R. Carver, and Kostas E. Bekris

***Abstract*— This paper aims to improve the computational efficiency of motion planning for mobile robots with non-trivial dynamics through the use of learned controllers. It adopts a decoupled strategy, where a system-specific controller is first trained offline in an empty environment to deal with the robot's dynamics. For a target environment, the proposed approach constructs offline a data structure, a "Roadmap with Gaps," to approximately learn how to solve planning queries in this environment using the learned controller. The nodes of the roadmap correspond to local regions. Edges correspond to applications of the learned control policy that approximately connect these regions. Gaps arise because the controller does not perfectly connect pairs of individual states along edges. Online, given a query, a tree sampling-based motion planner uses the roadmap so that the tree's expansion is informed towards the goal region. The tree expansion selects local subgoals given a wavefront on the roadmap that guides towards the goal. When the controller cannot reach a subgoal region, the planner resorts to random exploration to maintain probabilistic completeness and asymptotic optimality. The accompanying experimental evaluation shows that the approach significantly improves the computational efficiency of motion planning on various benchmarks, including physics-based vehicular models on uneven and varying friction terrains as well as a quadrotor under air pressure effects. Website: `https://prx-kinodynamic.github.io/projects/rogue`**

I. Introduction

Kinodynamic motion planning is useful for mobile robots with non-trivial dynamics that must negotiate environments with obstacles, such as a warehouse, or physical features like uneven terrain and ice. The problem is challenging when there is no access to a local steering function that can connect two robot states. Tree sampling-based kinodynamic planners [1] do not need a steering function as they only forward propagate the system's dynamics. Recent variants of these planners provide asymptotic optimality (AO) via the propagation of randomly sampled controls at every iteration [2]–[5]. The use of random controls, however, while important for theoretical properties, often results in slow convergence to high-quality solutions in practice.

This work aims to improve the efficiency of such planners using machine learning. Deep Reinforcement Learning (DRL) is a promising direction to improve the practical convergence of motion planners [6]. DRL can learn a local controller that approximately steers the robot between two states without collision. It can then be integrated inside a planner like a Probabilistic Roadmap (PRM) [7] or a Rapidly-exploring Random Tree (RRT) [8]. DRL is applicable in kinodynamic motion planning unlike some supervised learning alternatives [9]–[12], which require a steering function. DRL suffers, however, from large training data requirements and requires proper tuning of reward parameters [13].

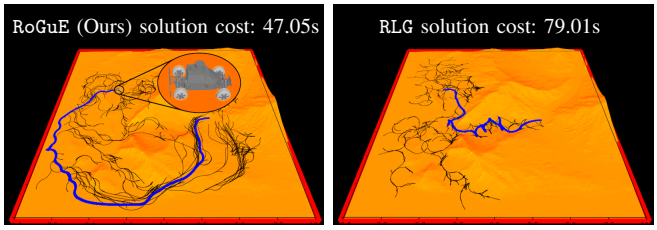

Fig. 1: Solution trajectories (thick lines) and planning trees (thin lines) for a MuSHR vehicle over an uneven terrain simulated in MuJoCo. The cost function is trajectory duration, which is impacted by the uneven terrain. The proposed expansion method for kinodynamic planning (left) leverages a roadmap with gaps to avoid difficult terrain resulting in shorter duration solutions. The alternative expansion (right), which samples random local goals, navigates the rough hills less effectively. It results in a shorter distance path but results in a much slower trajectory. Planning time was 60s for both methods for the computed trajectories.

Most current DRL solutions also lack long-horizon planning capabilities, meaning that a planner is still needed for the global search of the state space. Several recent works have leveraged DRL to build an abstract representation of the planning problem and search for an optimal path between the start and the goal on this representation. Search on the Replay Buffer (SoRB) [14] and Sparse Graphical Memory (SGM) [15] build a graph where the nodes correspond to states visited by the DRL agent during training. Similar to SoRB and SGM, Deep Skill Graphs [16]–[18] builds a graph representation, where nodes correspond to subgoals, and edges correspond to control policies between them. A common feature of these methods is that the control policy is trained in the planning environment of interest. This requires the learning algorithm to reason jointly about the system's dynamics and the obstacles present in the environment, which is challenging for second-order systems [19].

Prior work integrates DRL in kinodynamic motion planning via a decoupled strategy [20], [21], where a controller is first trained offline in an empty environment and the learning process only deals with the system's dynamics. The absence of obstacles allows learning the controller with significantly fewer data and only a sparse reward. During online planning, these prior efforts engineer local goals that bias expansion toward the global planning goal via manual engineering. The local goals are passed to the controller, which outputs a control towards them. Designing, however,

The authors are with the Dept. of Computer Science, Rutgers University, NJ, USA. E-mail: {as2578, kb572}@rutgers.edu. This work is partly supported by NSF NRT-FW-HTS award 2021628.

an informed local goal procedure requires manual effort, which is undesirable and may not apply equally well across environments. Furthermore, the local goals these procedures generate are unaware of the trained controller's reachability properties.

This work proposes a data structure, a **Roadmap with Gaps**, that learns the approximate reachability of local regions in a given environment given a controller. The approach constructs a directed graph in the free configuration space of the robot. An edge exists from a source node/region to a target when the source node's nominal state can reach the target node's termination set without collisions by application of the controller. Gaps arise since the learned controller does not connect any two exact states on this roadmap perfectly. Given a new planning problem in this environment, a wavefront expressing the cost-to-goal on this roadmap provides every node with the direction of motion towards the goal. This roadmap guidance is integrated with an AO tree sampling-based planner, where the accessible neighboring roadmap node with the lowest cost towards the global goal is selected as the expansion target for the tree planner.

The proposed approach provides a tradeoff. It incurs an offline computational cost for pre-processing a known environment and the robot's dynamics to provide online computational benefits for multiple planning queries in the same workspace. At the same time it retains AO properties and is an informed, efficient solution by understanding the reachability properties of the control method used for the target system and the environment's topology. Prior approaches that guide tree sampling-based planners using graphical abstractions [22], [23] do not provide desirable properties (e.g., AO) or do not reason about the system's dynamics. A related approach proposed *Bundle of Edges (BoE)* for kinodynamic planning [24] but relies on random control propagation, which reduces efficiency.

In summary, the paper's contributions are the following:

- It introduces the "Roadmap with Gaps," a data structure that provides high-level guidance how a robot can navigate a target environment given a (potentially learned) controller for the target robotic system.
- It adapts an existing framework for Asymptotically Optimal (AO) kinodynamic motion planning to utilize the "Roadmap with Gaps" and achieve improved efficiency. This results in the proposed **Ro**admap-**Gu**ided **E**xpansion (`RoGuE`)-Tree method.

The accompanying evaluation demonstrates the effectiveness of `RoGuE` both on analytically and physically simulated mobile robots in various environments, including physics-based vehicular models on uneven and varying friction terrains as well as a quadrotor under air pressure effects. `RoGuE` results in lower-cost solutions faster than random propagation given an AO sampling-based kinodynamic planner.

II. Preliminaries

Consider a system with state space $\mathbb{X}$ and control space $\mathbb{U}$. $\mathbb{X}$ is divided into collision-free ($\mathbb{X}_f$) and obstacle ($\mathbb{X}_o$) subsets. The dynamics $\dot{x} = f(x, u)$ (where $x \in \mathbb{X}_f, u \in \mathbb{U}$) govern the robot's motions. The process f can be an analytical ordinary differential equation (ODE) or modeled via a physics engine, e.g., MuJoCo [25]. A function $\mathbb{M} : \mathbb{X} \to \mathbb{Q}$ maps a state $x \in \mathbb{X}$ to its corresponding *configuration space* point $q \in \mathbb{Q}$ ($q = \mathbb{M}(x)$). The inverse mapping $\mathbb{M}^{-1}(q_i)$ returns a state $x_i \in \mathbb{X}$ by setting the dynamics term to some nominal value (e.g., by setting all velocity terms to 0). A distance function $d(\cdot, \cdot)$ is defined over $\mathbb{Q}$, which corresponds to a weighted Euclidean distance metric in SE(2).

A *plan* p_T is a sequence of piecewise-constant controls of duration T that induce a trajectory $\tau \in \mathcal{T}$, where $\tau : [0, T] \mapsto \mathbb{X}_f$. Given a start state $x_0 \in \mathbb{X}_f$ and a goal set $X_G \subset \mathbb{X}_f$, a feasible motion planning problem admits a solution trajectory of the form $\tau(0) = x_0, \tau(T) \in X_G$. The goal set is defined as $X_G = \{x \in \mathbb{X}_f \mid d(\mathbb{M}(x), q_G) < \epsilon\}$, or equivalently, $\mathcal{B}(q_G, \epsilon)$ where ϵ is a tolerance parameter. A heuristic $h : \mathbb{X} \to \mathbb{R}^+$ estimates the *cost-to-go* of an input state x to the goal region X_G. Each solution trajectory has a cost given by $\texttt{cost} : \mathcal{T} \to \mathbb{R}^+$. An optimal motion planning problem aims to minimize the cost of the solution trajectory.

Sampling-Based Planning Framework: The framework uses the forward propagation model f to explore $\mathbb{X}_f$ by incrementally constructing a tree via sampling in $\mathbb{U}$. Algo. 1 outlines the high-level operation of a sampling-based motion planner (Tree-SBMP) that builds a tree of states rooted at the initial state x_0 until it reaches X_G.

Algorithm 1: Tree-SBMP($\mathbb{X}, \mathbb{U}, x_0, X_G$)

```
1 T ← {x_0};
2 while termination condition is not met do
3     x_sel ← SELECT-NODE(T);
4     u ← EXPAND(x_sel);
5     x_new ← PROPAGATE(x_sel, u);
6     if (x_sel → x_new) ∈ X_f then
7         EXTEND-TREE(T, x_sel → x_new);
```

Each iteration of Tree-SBMP selects an existing tree node/state x_{sel} to expand (Line 3). Then, it generates a control sequence u and propagates it from x_{sel} to obtain a new state x_{new} (Lines 4-5). The resulting edge is added to the tree if not in collision (Lines 6-7). Upon termination (e.g., a time threshold), if the tree has states in X_G, the best-found solution according to *cost* is returned. By varying how the key operations in Algo. 1 are implemented, different variations can be obtained. The specific variant this work adopts is the informed and AO "Dominance-Informed Region Tree" (DIRT) [4]. It uses an admissible state heuristic function h to select nodes in an informed manner. If x_{new} improves upon x_{sel} given h, then it is selected as the next x_{sel}. DIRT also propagates a "blossom" of k controls at every iteration and prioritizes the propagation of the edge that brings the robot closer to the goal given the heuristic.

III. Proposed Method

The focus of this work is on line 4 of Algo. 1 above, i.e., how to generate the control that is expanded out of x_{sel}. In particular, the method computes first a local goal q_{lg} and propagates a control $u = \pi(x_{\text{sel}}, q_{\text{lg}})$ that progresses

towards that local goal given a controller π. The controller is first applied at the selected node $x_{\text{sel}} \in \mathbb{X}$ and generates a control sequence towards reaching the local goal q_{lg} without considering obstacles.

Overall, the proposed method has 2 offline stages: (i) training a controller $\pi(x, q)$ in an obstacle-free environment, and (ii) building a "Roadmap with Gaps" $(\mathcal{V}, \mathcal{E})$ in the target environment given the available controller. Finally, it has an online phase given a motion planning query (x_0, x_G) in the target environment. Online, a sampling-based kinodynamic planner expands a tree of feasible trajectories guided by a wavefront function computed over the "Roadmap with Gaps".

A. Training a Controller offline

A goal-conditioned controller $u = \pi(x, q)$ is first trained via reinforcement learning to reach from an initial state x to a goal set $\mathcal{B}(q, \epsilon)$, i.e., within an ϵ distance of q. For the training, this is attempted for any $(x, q) \in \mathbb{X} \times \mathbb{Q}$ in an empty environment of given dimensions. The training process collects transitions $(x_t, u_t, \mathcal{C}(x_t, q), x_{t+1}, q)$, which are stored in a replay buffer. The cost function $\mathcal{C} : \mathbb{X} \times \mathbb{Q} \rightarrow \{0, -1\}$ has a value of $\mathcal{C}(x_t, q) = 0$ iff $x_t \in \mathcal{B}(q, \epsilon)$, and -1 otherwise. During each iteration, mini-batches of transitions are sampled from the buffer. A Soft Actor-Critic (SAC) [26] algorithm is employed, which minimizes the total cost $\mathbb{E}_{x_0, q_G \sim \mathbb{X} \times \mathbb{Q}}[\sum_{t=0}^{T} \mathcal{C}(x_t, q_G)]$. Concurrently, Hindsight Experience Replay (HER) [27] relabels some transitions with alternative goals to provide additional training signals from past experiences.

B. Building a Roadmap with Gaps offline

The proposed approach then builds a "Roadmap with Gaps" $(\mathcal{V}, \mathcal{E})$ at the target environment, i.e., a graphical representation where nodes $\mathcal{V}$ correspond to configurations q_i of the vehicle. Edges $(q_i, q_j) \in \mathcal{E}$ exist between vertices as long as the application (of maximum duration $T_{\max}$) of the available controller $\pi(\mathbb{M}^{-1}(q_i), q_j)$ at a zero velocity state $\mathbb{M}^{-1}(q_i)$ of the initial configuration q_i brings the system within a hyperball $\mathcal{B}(q_j, \epsilon)$ of the configuration q_j.

The roadmap construction procedure (Fig 2a) samples first a set of configuration *milestones* $\{q_i\}_{i=1}^{|N|}$, which form the vertices $\mathcal{V}$ in the roadmap. In this work, the milestones are chosen over a grid in $\mathbb{Q}$. They are collision-checked and verified to be in $\mathbb{Q}_{\text{f}}$. Then, for the generation of edges $\mathcal{E}$, the procedure selects a random configuration $q_i \in \mathcal{V}$ and obtains two sets: A and D. A is the set of all vertices $q \in \mathcal{V}$, whose hyperballs $\mathcal{B}(q, \epsilon)$ can be reached from $x_i = \mathbb{M}^{-1}(q_i)$ given the controller π. Similarly, D is the set of vertices $q \in \mathcal{V}$, where the state $x = \mathbb{M}^{-1}(q)$ can reach the hyperball $\mathcal{B}(q_i, \epsilon)$ given the controller π. Then, edges from q_i to vertices in A and edges from vertices in D to q_i are added to the set $\mathcal{E}$.

The application of the controller for the edge construction, especially a learned one for a non-linear dynamical system, implies that for all edges (q_i, q_j) in the roadmap, there is no guarantee that the resulting configuration q_j can be achieved exactly from q_i. Instead, the corresponding edge only guarantees that the system will be within a hyperball $\mathcal{B}(q_G, \epsilon)$ if it is initialized at $\mathbb{M}^{-1}(q_i)$. Consequently, the edges of the roadmap introduce **"gaps"** as highlighted by the figure. This issue is exacerbated if the controller is used to follow a sequence of edges on the roadmap, e.g., (q_i, q_j) and (q_j, q_k). Since the controller's application over the first edge can only bring the system in the vicinity of q_j, the application of the controller corresponding to the second edge at the resulting configuration may not even bring the system within an ϵ-hyperball of q_k. Consequently, paths on the "Roadmap with Gaps" do not respect the dynamic constraints of the vehicle and cannot be used to directly solve kinodynamic planning problems. They can still provide, however, useful guidance for a kinodynamic planner.

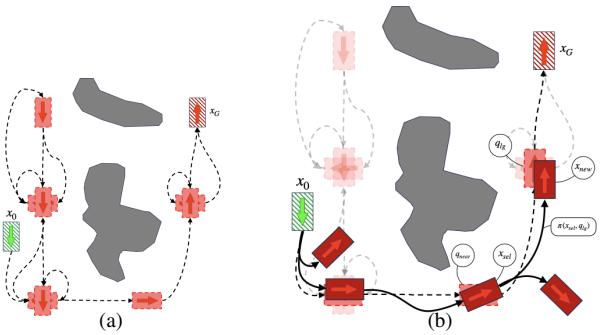

Fig. 2: (a) A *Roadmap with Gaps* consists of vertices (configurations, represented as dotted boxes). The roadmap's directional edges (dotted lines) correspond to where the controller was successfully executed from the source to the target configuration, given some tolerance. (b) For a new planning query (x_0, x_G), the start q_0 and goal q_G are added to the roadmap (transparent). Given the current planning tree (opaque), Roadmap-Guided Expansion (RoGuE) selects informed local goals for the controller π. The closest roadmap node q_{near} to the selected tree node x_{sel} is identified. Its successor is passed as the local goal q_{lg} to the controller. This expansion adds a new tree node x_{new}.

C. RoGuE: Guiding expansion via a roadmap with gaps

Algo. 2 describes the **Ro**admap-**Gu**ided **E**xpansion (RoGuE)-Tree method, which uses a "Roadmap with Gaps" to guide the online expansion of an AO Tree Sampling-based Motion Planner given a new query (x_0, x_G).

It first adds vertices $q_0 = \mathbb{M}(x_0)$ and $q_G = \mathbb{M}(x_G)$ to $\mathcal{G}$. Then, it adds edges from q_0 to all vertices accessible from it, i.e., the set of all vertices $q_i \in \mathcal{V}$ such that applying the controller from x_0 for maximum duration $T_{\max}$ returns a collision-free trajectory τ with $\mathbb{M}(\tau.\text{end}()) \in \mathcal{B}(q_i, \epsilon)$. Similarly, it adds edges to q_G from all vertices that can access the goal set X_G.

A *wavefront function* $\mathcal{W} : \mathcal{V} \mapsto \mathbb{R}^+$ is computed over the vertices of the roadmap. Initially, the wavefront value for all vertices is set to infinity. Then, the wavefront value of the goal $(\mathcal{W}(q_G))$ is set to zero, and a backward search is performed. Given the wavefront, every vertex in $\mathcal{V}$ now has the notion of a *successor* associated with it, defined to be its

out-neighbor with minimum $\mathcal{W}$ value, i.e., $\texttt{Successor}(v) = \arg\min_{\mathcal{V}}\{\mathcal{W}(v') \mid (v, v') \in \mathcal{E}\}$. For a node with an infinite cost-to-goal (because the roadmap does not provide it with a path to the goal), its successor is undefined.

Algorithm 2: RoGuE-Tree $(\mathbb{X}, \mathbb{U}, x_0, x_G, \pi, (\mathcal{V}, \mathcal{E}))$

```
1  Add q_0, q_G to roadmap (V, E) as start and goal;
2  W ← GET-WAVEFRONT((V, E));
3  T ← {x_0};
4  while termination condition is not met do
5  |   x_sel ← SELECT-NODE(T);
6  |   u ← RoGuE(x_sel, V, W, π);
7  |   x_new ← PROPAGATE(x_sel, u);
8  |   if (x_sel → x_new) ∈ X_f then
9  |   |   EXTEND-TREE(T, x_sel → x_new);
```

RoGuE (Algo. 3, Fig 2b) is an expansion procedure that uses the roadmap wavefront information $\mathcal{W}$ to provide an informed local goal to π. The first time a tree node x_{sel} is selected for expansion, RoGuE identifies the closest roadmap node $q_{\text{near}} \in \mathcal{V}$ according to the distance function $d(\cdot, \cdot)$ (Line 2). It then queries the $\texttt{Successor}(q_{\text{near}})$ given the wavefront $\mathcal{W}$. If (q_{near}) is defined, it is provided as the local goal q_{lg} to the controller π (Lines 3-5). If the successor is not defined, a random local goal in $\mathbb{Q}$ is provided (Line 6-7).

Algorithm 3: RoGuE $(x_{\texttt{sel}}, \mathcal{V}, \mathcal{W}, \pi)$

```
1  if first time x_sel is expanded then
2  |   q_near ← ClosestRoadmapNode(x_sel, V);
3  |   q_lg ← Successor(q_near, W);
4  |   if q_lg is defined then
5  |   |   u ← π(x_sel, q_lg);
6  |   else
7  |   |   u ← π(x_sel, Q.sample());
8  else
9  |   u ← U.random-sample();
10 return u;
```

Following the informed operation of the DIRT planner [4], when the roadmap cost-to-go value of a node is lower than that of its parent's, then the child node is immediately reselected for expansion so that the tree can continue to make progress along a promising path of the roadmap with gaps.

All (start, goal) pairs in the accompanying experiments below are included as milestones during the roadmap construction to reduce connection time during online planning. Alternatively, the connection of start and goal configurations to the roadmap lends itself to multi-threaded implementations. Or, similarly to the "roadmap cost-to-go" value definition in Line 2 of Alg. 3, the closest roadmap nodes can be used as surrogates for the corresponding start and goal states.

Maintaining Asymptotic Optimality: As long as all tree nodes have a non-zero probability of being selected for expansion, and the probability of an expansion being successful from a node along the lowest-cost trajectory is non-zero, the sampling-based tree planner remains AO. The node selection process of RoGuE adopts that of the DIRT planner [4], which, while informed, maintains a positive probability for all tree nodes. Similarly, while RoGuE employs an initial set of informed expansions from each node (given the roadmap information), subsequent expansions apply random controls from the set $\mathbb{U}$ (Algo 3, Line 8-9). In this way, the approach retains the AO properties of DIRT [4].

In practice, when the informed processes of RoGuE guide the selection and expansion of nodes along high quality solutions, the method achieves an improved convergence rate relative to alternatives that do not have access to the roadmap information as the experimental evaluation below shows. Showing this improvement in convergence rate is an objective of future research efforts for this line of work.

IV. Experimental Evaluation

The **robot systems** considered in the evaluation are: (i) an analytically simulated second-order differential-drive, (ii) an analytically simulated car-like vehicle (where $\texttt{dim}(\mathbb{X}) = 5, \texttt{dim}(\mathbb{U}) = 2$), (iii) a MuSHR car [28] physically simulated using MuJoCo [25] ($\texttt{dim}(\mathbb{X}) = 27, \texttt{dim}(\mathbb{U}) = 2$), and (iv) a Skydio X2 Autonomous Drone ($\texttt{dim}(\mathbb{X}) = 13, \texttt{dim}(\mathbb{U}) = 4$). For the drone, the distance function $d(\cdot, \cdot)$ operates over the (x, y, z) of its center of mass. For all systems, the parameter ϵ is set to the same value 0.5. All planning experiments are implemented using the ML4KP software library [29] and executed on a cluster with Intel(R) Xeon(R) Gold 5220 CPU @ 2.20GHz and 512 GB of RAM.

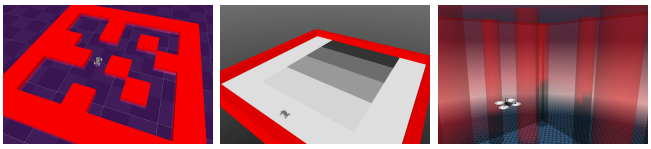

Fig. 3: Physically simulated benchmarks using MuJoCo. (L-R) Maze, Friction, Quadrotor.

Across experiments, the following **metrics** are measured for every planner: (1) Average normalized cost of solutions found over time, and (2) Ratio of experiments for which solutions were found over time. For all planning problems, the path cost is defined as the solution plan's duration. To better reflect the performance of different methods and account for the difficulty of different planning problems, path costs discovered by a method on each planning problem are normalized by dividing by the best path cost ever found for a problem across all planners.

Two **comparison expansion functions** are considered in the evaluation: (a) Random uses a blossom expansion of random controls in $\mathbb{U}$, and (b) RLG samples Random Local Goals as input to π and outputs the controls returned. In terms of **comparison motion planners**, both an uninformed Rapidly-exploring Randomized Tree (RRT) [1] and the informed, AO DIRT planners are considered. For the Random and RLG expansion strategies of DIRT, a blossom of 5 controls is implemented.

Additional AO planners were considered for experimentation but it was difficult to provide useful results for them. The *Bundle of Edges (BoE)* [24] approach failed to find solutions while using a similarly-sized roadmap. The *discontinuity-bounded A** (dbA*) [30] relies on motion primitives, which are not available, however, for the robots in the experiments of this paper as they exhibit second-order dynamics. It is not trivial for them to acquire effective motion primitives.

A. Results on analytically simulated benchmarks

In these experiments, the performance of the expansion functions is measured on three sets of planning benchmarks for the analytically simulated vehicular systems: (a) 8 problems in an environment with `Narrow` passages, (b) 6 problems in the `Indoor` environment from Arena-bench [31], and (c) 8 problems in the `Warehouse` environment from Bench-MR [32]. Figure 4 provides the numerical results.

Across all benchmarks, for the differential drive and car-like dynamics, `DIRT-RoGuE` finds the lowest cost solutions overall. It also is the only expansion strategy that returns solutions in all trials. Among the RRT expansion strategies, `RRT-RoGuE` achieves the highest success rate across all benchmarks and the lowest cost solutions overall. `RRT-RoGuE` also achieves comparable performance (both in terms of success rate and solution quality) to the informed `DIRT-Random` an `DIRT-RLG` planners.

Comparison to Kinematic Planning and Path Following: A naïve alternative to the proposed solution is to use the configurations along a path on the roadmap as consecutive local goals for a path following controller. For the car-like system, a pose-reaching controller [33] was employed to drive the robot to a given pose $\begin{pmatrix} v \\ \omega \end{pmatrix} = \begin{pmatrix} k_\rho \rho \\ k_\alpha \alpha + k_\beta \beta \end{pmatrix}$, where each k parameter is a gain term, ρ and α are the distance and bearing to the local goal respectively, and β is the angle difference between α and the current angle. The controller is tested on paths retrieved from the Roadmap with Gaps for the benchmarks of Fig 4. Only 2 such executions, however, returned collision-free trajectories. This is due to (a) the environments containing multiple narrow passages and (b) the paths returned by the roadmap still contain "gaps" that the controller cannot easily negotiate. This motivates the proposed solution and alternatives that are similarly obstacle-aware and which reason about the robot's dynamics.

B. Results on physically simulated benchmarks

The performance of the expansion functions is measured on the following benchmarks for MuSHR: (a) navigating a `Maze` from `D4RL` [34], (b) an environment with uneven `Terrain` features [35], (c) and an environment with different friction values (`Friction`). Note that the controller is trained in an empty environment with flat terrain and friction. The roadmap captures the traversability of different parts of the environment using the controller. In the `Quadrotor` benchmark, the X2 drone must navigate an indoor environment with pillars and air pressure effects.

Figs. 1 and 3 visualize the different environments in MuJoCo, and Fig. 5 provides the experimental results. Only the DIRT motion planner is reported in these experiments as the RRT-based solutions cannot find a solution within the allotted times. Since each call to the MuJoCo engine is expensive, all expansion strategies use a blossom $k = 1$.

`RoGuE` finds the lowest cost solution across all benchmarks. Both `Random` and `RLG` consistently fail to find solutions across trials. Using the learned controller in `RLG` does lead to improved solution quality relative to `Random`. In both the `Maze` and `Friction` benchmarks, `RoGuE` leverages the Roadmap with Gaps to find solutions across trials quickly. `RoGuE` also returned the most solutions in the `Terrain` benchmark given the same planning budget. In the `Quadrotor` benchmark, `RoGuE` is the only expansion method that discovers any solutions due to the tight placement of obstacles and the speed of the X2 drone.

Comparison to Deep RL solutions: Table I evaluates two purely DRL-based strategies trained on the benchmarks of Fig 5 in terms of success rate `Succ`, as well as offline cost (`Offl`, in terms of # of calls made to the MuJoCo engine). The offline cost of the DRL methods is reported when their best performance is observed, and the success rate does not improve after training for longer. The online costs `Onl` for the sampling-based planners are also reported. The online cost for the RL solutions is minimal. `SAC+HER` trains a goal-conditioned controller $u = \pi(x, q)$ directly in the planning environment. The approach achieves a low success rate relative to the proposed kinodynamic planning solution. The low success on `Quadrotor` can be attributed to the difficulty in jointly learning the dynamics and obstacle avoidance. Due to simpler dynamics, the performance is better on the `Maze` and `Friction` benchmarks. `H-SAC+HER` follows a hierarchical approach similar to `RoGuE` by training a policy to predict local goals for the controller to reach at every step, i.e., $q_{\text{lg}} = \phi(x)$. This slightly improves the success rate relative to `SAC+HER` on `Quadrotor`. The success rate is comparable to `SAC+HER` in the `Maze` environment, while it is lower on `Friction`. This indicates the difficulty of DRL strategies in learning an informed local goal procedure, which the Roadmap with Gaps captures via offline computation.

V. Conclusion

This paper proposes a strategy that can benefit from learned controllers to improve the efficiency of kinodynamic planning for robots with significant dynamics. It utilizes a controller trained offline for a robot in an empty environment. The target environment is represented via a "Roadmap with Gaps" over local regions and applications of the controller between them. Given a wavefront over the roadmap for a specific goal, a tree sampling-based motion planner generates informed subgoals and uses the controller to reach them. When the controller cannot reach a subgoal, the planner resorts to random exploration. Experiments on various benchmarks demonstrate significant improvement in planning efficiency.

For higher-dimensional systems, the memory requirements of the roadmap can be improved by considering sparse representations similar to geometric planning [36]. Furthermore,

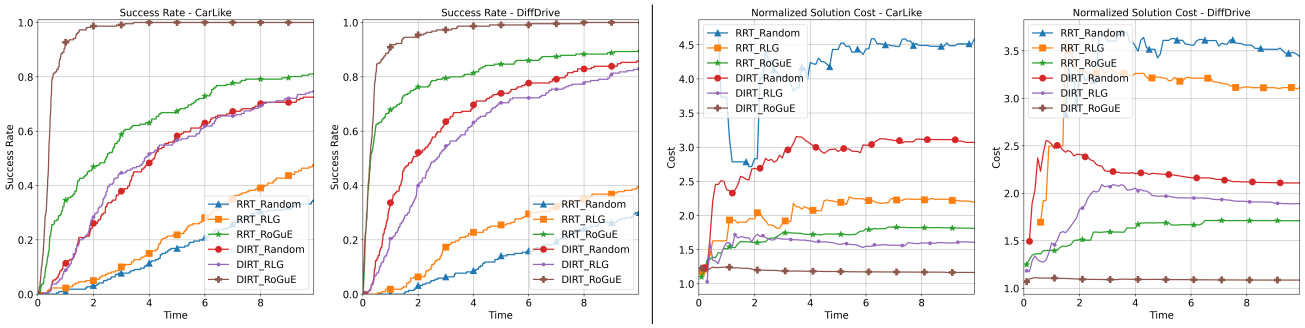

Fig. 4: Evaluation on the analytically simulated benchmarks. Left and middle-left: higher success rate earlier is better. Right and middle-right: lower path cost is better. As more solutions are discovered, additional solutions for harder problems are discovered, so in some cases, the average cost may increase over time. Each problem instance is run 10 times to account for different random seeds.

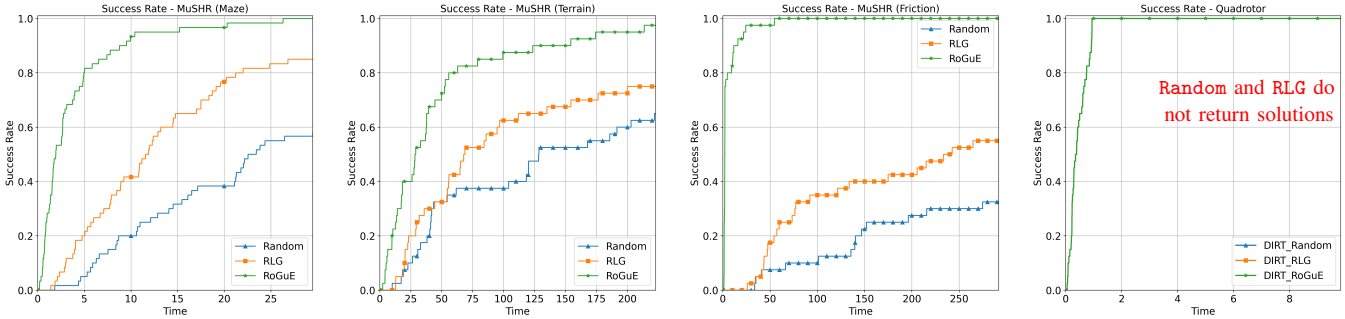

(a) Success rates of the planners on each physically simulated benchmark. Higher success rate earlier is better.

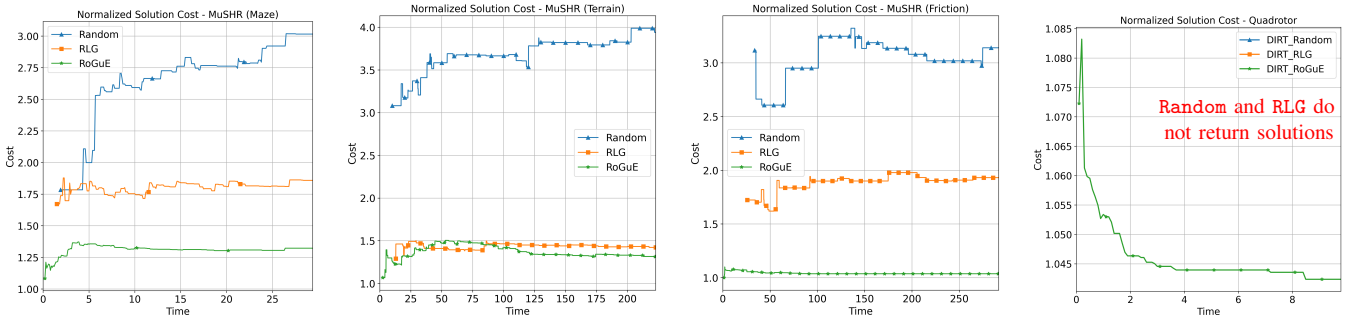

(b) Solution quality of the planners on the physically simulated benchmarks. Lower values are better. As more solutions are discovered, harder instances are resolved, so in some cases, the average cost may increase over time.

Fig. 5: Evaluation on the physically simulated systems via MuJoCo. Each instance is executed 10 times with different random seeds. For the `Quadrotor`, the `Random` and `RLG` strategies consistently fail to return solutions and hence their results are not displayed.

	RoGuE			SAC+HER		H-SAC+HER		Random		RLG		
Benchmark	Offl	Onl	Succ	Offl	Succ	Offl	Succ	Onl	Succ	Offl	Onl	Succ
Friction	2.5M	58.15	**100%**	0.81M	35%	1.48M	13%	295.225	37.5%	1M	609.225	60%
Maze	2.05M	241.62	**100%**	0.54M	34%	1.74M	31%	623.57	58%	1M	693.73	87%
Quadrotor	1M	736.3	**100%**	1.3M	5%	1.01M	13%	14k	0%	100k	13.7k	0%

TABLE I: Comparing DRL approaches against SBMPs in terms of computation costs (# of calls made to the physics engine) and success rate on the physically-simulated benchmarks.

learned reachability estimators can assist in efficient roadmap construction and online queries. This work assumes that an accurate model of the environment and the vehicular system is available, which complicates the direct deployment of the proposed approach on real vehicular systems. This also motivates integrating the proposed motion planner with system identification tools as well as state estimation and feedback control to track the planned trajectory.

REFERENCES

[1] S. M. LaValle and J. J. Kuffner Jr, "Randomized kinodynamic planning," *IJRR*, vol. 20, no. 5, pp. 378–400, 2001.

[2] Y. Li, Z. Littlefield, and K. E. Bekris, "Asymptotically optimal sampling-based kinodynamic planning," *IJRR*, vol. 35, no. 5, pp. 528–564, 2016.

[3] K. Hauser and Y. Zhou, "Asymptotically optimal planning by feasible kinodynamic planning in a state–cost space," *T-RO*, vol. 32, no. 6, pp. 1431–1443, 2016.

[4] Z. Littlefield and K. E. Bekris, "Efficient and asymptotically optimal kinodynamic motion planning via dominance-informed regions," in *IROS*, 2018.

[5] M. Kleinbort, E. Granados, K. Solovey, R. Bonalli, K. E. Bekris, and D. Halperin, "Refined analysis of asymptotically-optimal kinodynamic planning in the state-cost space," in *ICRA*, 2020.

[6] T. McMahon, A. Sivaramakrishnan, E. Granados, and K. E. Bekris, "A survey on the integration of machine learning with sampling-based motion planning," *Foundations and Trends® in Robotics*, vol. 9, no. 4, pp. 266–327, 2022.

[7] A. Faust, O. Ramírez, M. Fiser, K. Oslund, A. Francis, J. O. Davidson, and L. Tapia, "PRM-RL: Long-range robotic navigation tasks by combining reinforcement learning and sampling-based planning," *ICRA*, 2018.

[8] H.-T. L. Chiang, J. Hsu, M. Fiser, L. Tapia, and A. Faust, "RL-RRT: Kinodynamic motion planning via learning reachability estimators from RL policies," *RA-L*, vol. 4, no. 4, pp. 4298–4305, 2019.

[9] Y. Li, R. Cui, Z. Li, and D. Xu, "Neural network approximation based near-optimal motion planning with kinodynamic constraints using RRT," *IEEE Transactions on Industrial Electronics*, vol. 65, pp. 8718–8729, 2018.

[10] G. P. Kontoudis and K. G. Vamvoudakis, "Kinodynamic motion planning with continuous-time q-learning: An online, model-free, and safe navigation framework," *IEEE transactions on neural networks and learning systems*, vol. 30, no. 12, pp. 3803–3817, 2019.

[11] J. J. Johnson, L. Li, F. Liu, A. H. Qureshi, and M. C. Yip, "Dynamically constrained motion planning networks for non-holonomic robots," in *IROS*, 2020, pp. 6937–6943.

[12] L. Li, Y. Miao, A. H. Qureshi, and M. C. Yip, "Mpc-mpnet: Model-predictive motion planning networks for fast, near-optimal planning under kinodynamic constraints," *RA-L*, vol. 6, no. 3, 2021.

[13] Z. Xu, B. Liu, X. Xiao, A. Nair, and P. Stone, "Benchmarking reinforcement learning techniques for autonomous navigation," in *ICRA*, 2023.

[14] B. Eysenbach, R. R. Salakhutdinov, and S. Levine, "Search on the replay buffer: Bridging planning and reinforcement learning," *NeurIPS*, 2019.

[15] S. Emmons, A. Jain, M. Laskin, T. Kurutach, P. Abbeel, and D. Pathak, "Sparse graphical memory for robust planning," *NeurIPS*, 2020.

[16] A. Bagaria and G. Konidaris, "Option discovery using deep skill chaining," in *ICLR*, 2019.

[17] A. Bagaria, J. K. Senthil, M. Slivinski, and G. Konidaris, "Robustly learning composable options in deep reinforcement learning." in *IJCAI*, 2021.

[18] A. Bagaria, J. K. Senthil, and G. Konidaris, "Skill discovery for exploration and planning using deep skill graphs," in *International Conference on Machine Learning*. PMLR, 2021, pp. 521–531.

[19] R. Strudel, R. Garcia, J. Carpentier, J.-P. Laumond, I. Laptev, and C. Schmid, "Learning obstacle representations for neural motion planning," in *CoRL*, 2020.

[20] A. Sivaramakrishnan, E. Granados, S. Karten, T. McMahon, and K. E. Bekris, "Improving kinodynamic planners for vehicular navigation with learned goal-reaching controllers," in *IROS*, 2021.

[21] T. McMahon, A. Sivaramakrishnan, K. Kedia, E. Granados, and K. E. Bekris, "Terrain-aware learned controllers for sampling-based kinodynamic planning over physically simulated terrains," in *IROS*, 2022.

[22] D. Le and E. Plaku, "Guiding sampling-based tree search for motion planning with dynamics via probabilistic roadmap abstractions," in *IROS*, 2014.

[23] M. G. Westbrook and W. Ruml, "Anytime kinodynamic motion planning using region-guided search," in *IROS*, 2020.

[24] R. Shome and L. E. Kavraki, "Asymptotically optimal kinodynamic planning using bundles of edges," in *ICRA*, 2021.

[25] E. Todorov, T. Erez, and Y. Tassa, "Mujoco: A physics engine for model-based control," in *IROS*, 2012.

[26] T. Haarnoja, A. Zhou, P. Abbeel, and S. Levine, "Soft actor-critic: Off-policy maximum entropy deep reinforcement learning with a stochastic actor," in *ICML*, 2018.

[27] M. Andrychowicz, D. Crow, A. Ray, J. Schneider, R. H. Fong, P. Welinder, B. McGrew, J. Tobin, P. Abbeel, and W. Zaremba, "Hindsight experience replay," in *NeurIPS*, 2017.

[28] S. S. Srinivasa, P. Lancaster, J. Michalove, M. Schmittle, C. Summers, M. Rockett, J. R. Smith, S. Chouhury, C. Mavrogiannis, and F. Sadeghi, "MuSHR: A low-cost, open-source robotic racecar for education and research," *CoRR*, vol. abs/1908.08031, 2019.

[29] E. Granados, A. Sivaramakrishnan, T. McMahon, Z. Littlefield, and K. E. Bekris, "Machine learning for kinodynamic planning (ml4kp)," https://github.com/PRX-Kinodynamic/ML4KP, 2021–2022.

[30] W. Hönig, J. Ortiz-Haro, and M. Toussaint, "db-a*: Discontinuity-bounded search for kinodynamic mobile robot motion planning," in *IROS*, 2022.

[31] L. Kästner, T. Bhuiyan, T. A. Le, E. Treis, J. Cox, B. Meinardus, J. Kmiecik, R. Carstens, D. Pichel, B. Fatloun, *et al.*, "Arena-bench: A benchmarking suite for obstacle avoidance approaches in highly dynamic environments," *RA-L*, vol. 7, no. 4, 2022.

[32] E. Heiden, L. Palmieri, L. Bruns, K. O. Arras, G. S. Sukhatme, and S. Koenig, "Bench-mr: A motion planning benchmark for wheeled mobile robots," *RA-L*, vol. 6, no. 3, 2021.

[33] P. I. Corke, W. Jachimczyk, and R. Pillat, *Robotics, vision and control: fundamental algorithms in MATLAB*. Springer, 2011, vol. 73.

[34] J. Fu, A. Kumar, O. Nachum, G. Tucker, and S. Levine, "D4rl: Datasets for deep data-driven reinforcement learning," 2020.

[35] K. Stachowicz, A. Bhorkar, D. Shah, I. Kostrikov, and S. Levine, "FastRLAP: A System for Learning High-Speed Driving via Deep RL and Autonomous Practicing," 2023. [Online]. Available: TODO

[36] A. Dobson and K. E. Bekris, "Sparse roadmap spanners for asymptotically near-optimal motion planning," *IJRR*, vol. 33, no. 1, pp. 18–47, 2014.